Dispersive microwave bifurcation of a superconducting resonator cavity incorporating a Josephson junction

E. Boaknin, V. Manucharyan, S. Fissette,* M. Metcalfe, L. Frunzio,
R. Vijay, I. Siddiqi,† A. Wallraff,‡ R. J. Schoelkopf, and M. Devoret

Department of Applied Physics, Yale University, New Haven, CT, USA

(Dated: February 19, 2007)

We have observed the dynamical bistability of a microwave superconducting Fabry-Perot cavity incorporating a non-linear element in the form of Josephson tunnel junction. The effect, which is the analog of optical bistability, manifests itself in the transmission and reflection characteristics of the cavity and is governed by a competition between the wave amplitude dependence of the resonant frequency and the finite residence time of the field energy inside the cavity. This finite residence time is solely due to extraction of radiation from the cavity by the measurement process. The tight quantitative agreement with a simple model based on the Duffing oscillator equation shows that the nonlinearity, and hence the bifurcation phenomenon, is solely dispersive.

Amplifying in the microwave frequency domain signals whose energy are at or close to the quantum limit constitute an experimental challenge whose pursuit is justified both by the fundamental understanding of amplification mechanisms in general [1] and by applications in radioastronomy [2] and quantum information processing [3]. One practical, minimal noise amplification mechanism involves pumping a purely dispersive non-linear medium in the vicinity of a bifurcation between two dynamical states. The weak input signals can then be detected either in the non-hysteretic regime for continuous, phase preserving operation or in the hysteresis regime where the medium provides latching by switching from one state to the other.

In this Letter, we demonstrate that a microwave superconducting cavity incorporating a Josephson junction can display a bistable regime of operation suitable for ultra-low noise amplification. The bifurcation associated with this bistability involves a dispersive non-linear dynamical evolution of the fields of the cavity on time scales given by its quality factor rather than a slow change in its parameters due to dissipation induced heating of the cavity material. Importantly, we show that the strength of the non-linearity depends on the combination of simple electrical characteristics of the junction and the cavity, both being entirely controllable by fabrication. The abscence of dissipation inside the cavity ensures that a minimal number of modes are involved in the amplification process, a necessary condition for amplification at the quantum limit [4]

A Josephson tunnel junction constitutes the only radio-frequency (RF) electrical element which is both non-dissipative and non-linear at low temperatures and whose characteristics are engineerable in a wide parameter range. This property makes it unique for applications in ultra-low noise amplifiers, particle detectors, and more recently, quantum information processing. The pioneering work on squeezing of Yurke *et. al.* in the 80's [5] had already showed that the Josephson junction could achieve for microwave radiation in the quantum regime what non-linear media could achieve for quantum optics. Since then, recent works in which a Josephson circuit is coupled to a superconducting microwave cavity have demonstrated that the strong-coupling regime of cavity QED in atomic physics could be attained [6]. Here, we are showing that the cavity can become so non-linear that the analog of dispersive optical bistability with atomic ensembles [7] can be observed.

In Fig. 1a we show our superconducting Fabry-Perot cavity constructed from a coplanar waveguide transmission line by interrupting the conductor with two in-plane capacitors playing the role of partially transparent mirrors (see Fig. 1b, d). The geometric distance between the capacitors determines the lowest resonance frequency of this resonator. In our experiments, by varying the length of the transmission line, the frequency is tuned between 1.5 and 10 GHz. The quality factor Q of the cavity was in the 400-2500 range and was entirely determined by the loading through the coupling capacitances. In a separate experiment[8] we have demonstrated that the contribution of intrinsic dissipation to Q for this type of resonator at our working temperatures ($T \sim 300$ mK) were negligible. In the middle of the cavity, the central conductor of the transmission line is interrupted with a gap into which a Al-AlOx-Al Josephson junction is inserted (see Fig. 1c), ensuring maximum coupling between the junction and odd cavity modes. Fabrication of the junction involves standard e-beam lithography, shadow mask evaporation and lift-off. Good metallic contacts between the leads of the junction and the Nb resonator were obtained with ion beam cleaning prior to the e-beam evaporation of aluminium films. In the following, we will concentrate on the lowest order mode for which the analysis developed in [11] applies.

The circuit diagram of our experiment is given in Fig. 1e where the two sections of loss-less coaxial
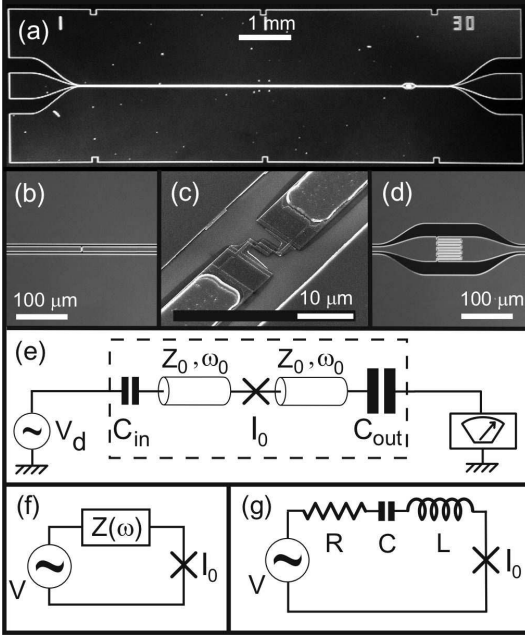
FIG. 1: (a) "Dark field" photographs of a chip sample showing the coplanar waveguide Nb resonator implementing a superconducting Fabry-Perot cavity on chip. Asymmetric finger capacitors (b)-(d) play the role of partially reflective mirrors. Non–dissipative non-linearity is provided a shadow-mask evaporated Josephson junction (c). (e) Schematic of the microwave circuit of the experiment. The dashed box surrounds the parts which are on-chip. Viewed from the Josephson junction the RF biasing circuit appears (f) as an impedance $Z(\omega)$ in series with a voltage source. (g) In the vicinity of the first mode of the resonator, the electromagnetic environment of the junction can be modeled by an LCR combination.
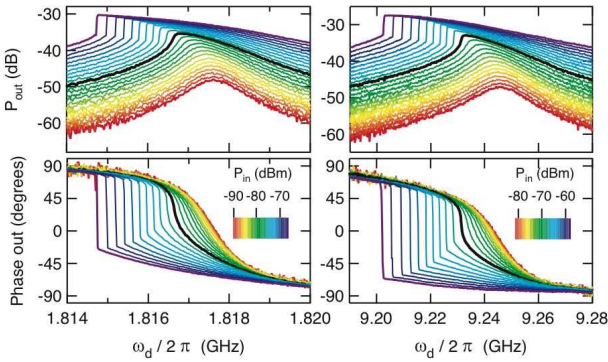

FIG. 2: Measured output power (top) and phase (bottom) of transmitted signal as a function of increasing drive frequency for a range of incoming powers (colors) and for samples 2 (left) and 3 (right). The black line corresponds to the critical power, separating the single state solution regime from the bistable one. The transition between states appears as a vertical jump.
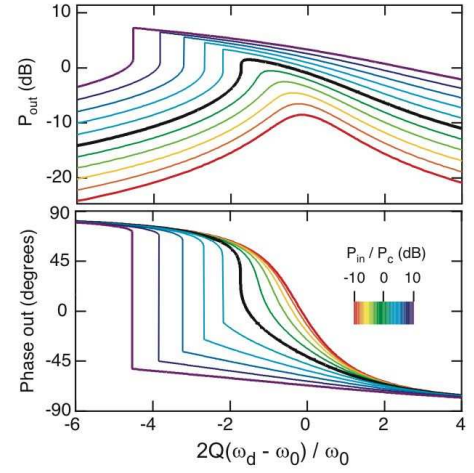

FIG. 3: Theoretical predictions corresponding to the protocol of Fig. 2 and calculated for the Duffing model, plotted as a function of reduced drive frequency $2Q(\omega_d - \omega_0)/\omega_0$.

transmission lines represent the coplanar waveguide on each side of the junction. The transmission lines are parametrized by a characteristic impedance ($Z_0 \sim 50\ \Omega$) and a frequency ω_0 corresponding to their $\lambda/2$ (fundamental) resonance. The small input capacitor C_{in} couples in a source signal from a microwave generator while the large output capacitor C_{out} couples out the transmitted signal to the first stage of our amplifier chain. A factor of 20 to 35 in capacitor asymmetry ensures that all the power escaping from the resonator is collected on the amplifier side. This maximizes the signal to noise ratio of the experiment since it prevents the input port to participate in the dissipation. Applying the Norton-Thevenin theorem, our microwave circuit can be seen from the junction as an ideal RF voltage generator connected to a series combination of the junction and a finite linear embedding impedance $Z(\omega)$ (see Fig. 1f). For drive frequencies in the vicinity of the fundamental mode the system is very well described by the model shown on Fig. 1g, where $Z(\omega)$ is now a series LCR circuit. When combined with the junction non-linear inductance governed by the parameter $L_J = \varphi_0/I_0$, where $\varphi_0 = \hbar/2e$, this circuit yields an equation, analogous to the Bloch-Maxwell equations described in ref [9], and which can be analyzed in detail [11]. In the asymmetric mirrors limit parameters of the circuit from Fig. 1 are given by $V = Z_0\omega_0 C_{in}V_d$, $R = Z_0^2 R_L \omega_0^2 C_{out}^2$, $L = \frac{Z_0}{4\ \omega_0/2\pi}$, $C = \frac{1}{\pi^2 Z_0\ \omega_0/2\pi}$ where R_L is the 50 Ω load resistance. Note that ω_0 absorbs a slight renormalization by the coupling capacitors. The quality factor is given by $Q = \frac{\pi}{2Z_0 R_L \omega_0^2 C_2^2}$. We will come back to this model after examining the data.

The basic principle of our experiment is to measure the transmission characteristics of the cavity as a function of both frequency and power. We studied three different chip samples for which the relevant parameters

are given in Table I. They were anchored to the final T=300 mK stage of a ^{3}He refrigerator. While we have mainly conducted CW measurements, we have also conducted measurements in which, keeping the frequency fixed, the power is ramped sufficiently rapidly to probe the internal dynamics of the cavity. Since we would like to demonstrate that the cavity is strongly non-linear even for small radiative energies stored inside it, the challenge of the experiment is to perform precise transmission measurements at very low power. A vector network analyzer sends a CW microwave signal on the small capacitor side and analyzes the transmitted signal coming out from the large capacitor side, after they have passed through the amplifier chain which includes one cryogenic HEMT amplifier at 4 K and two circulators placed at 300 mK and 4 K.

In Fig. 2 we show the typical transmitted signal amplitude (top panels) and phase (bottom panels) as a function of drive frequency for different input drive power and for two resonator frequencies (samples 2 and 3). The drive frequency was swept in 800 ms. At low drive power $P_{in} = \frac{1}{2R_L}V_d^2$ the response of the resonator is a Lorentzian centered on the resonator frequency. As drive power is increased, the resonant response sharpens on the low frequency side and softens on the high frequency side. At a critical drive power $P_{in} = P_c$, the maximum slope on the low frequency side diverges. Upon increasing the drive power further, a abrupt transition develops, whose position shifts to lower frequency with increasing power. The two panels of Fig. 2 demonstrate that the phenomenon presents itself in identical manners for two resonators despite their different resonant frequencies and quality factors. For clarity the response at the critical power is highlighted in black. At even higher drive power (data not shown), the system becomes chaotic as described elsewhere [10].

These results should be fully governed by the static solutions of the Duffing oscillator as described in [11]. Indeed, simple analytical relations for the transmitted power and phase at different drive powers show excellent qualitative agreement with the measurements as shown in Fig. 3. We now focus on the locations in the (ω_d, P_{in}) plane where the susceptibility is maximum, i.e. locations where $dP_{out}/d\omega_d$ is maximum. When $P_{in} > P_c$, these should correspond with the bifurcation points. We will also follow the point of maximum P_{out}. These results are plotted for the three samples and three different values of the DC critical current of the Josephson junctions patterned in our samples. We plot them against the reduced frequency $\Omega \equiv 2Q(\omega_0 - \omega_d)/\omega_0$ and P_{in}/P_c, both obtained independently for each sample. As expected, the various experimental points fall on a universal theoretical curve when properly scaled. Based on [11] we expect the bifurcation power to be given by $P_b(\Omega)/P_c = \frac{1}{12\sqrt{3}}\Omega^3(1 + 9/\Omega^2 \mp (1 - 3/\Omega^2)^{2/3})$ (blue and red lines respectively) and the power of highest derivative

		sample 1	sample 2	sample 3
measured	ω_0(GHz)	1.828	1.8177	9.246
	Q	2360	1500	460
	C_{in}(pF)	2.3 ± 0.2	1.5 ± 0.5	1.0 ± 0.1
	P_c(dBm)	-85.5 ± 1	-76.5 ± 1	-70 ± 1.5
inferred	L (nH)	6.7	6.8	1.3
	C (pF)	1100	1100	200
	R (Ω)	0.034	0.053	0.17
	I_0 (μA)	1.6 ± 0.2	1.5 ± 0.5	2.9 ± 0.35
expected	I_0 (μA)	1.3 ± 0.1	1.6 ± 0.1	3.35 ± 0.15

TABLE I: Table showing the measured values of parameters for samples studied in experiment, as well as inferred and expected parameters. C_{in} is obtained either from the measurement of other identical resonators with no Josephson junctions (samples 1 and 2) or by measuring the ratio of input and output powers leading to criticality and assuming that the quality factor is set by C_{out} (sample 3).
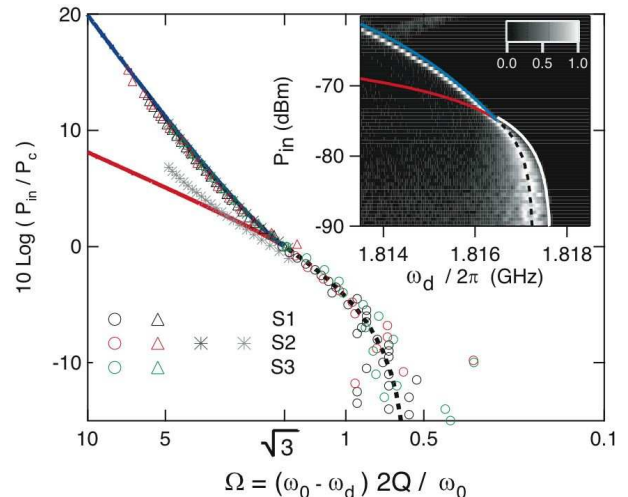

FIG. 4: Logarithmic plot of the highest derivative $dP_{out}/d\omega_d$ as a function of reduced parameters Ω and P_{in}/P_c. Lines depict theoretical prediction for the Duffing model. Triangles, circles and crosses represent respectively the measured bifurcation power, its highest derivative (below P_c), and the data of the hysteresis measurement. *Inset:* derivative of the output power with respect to drive frequency, normalized to its maximum as a function of drive frequency and power. Note the white line delimits the point where the output power is maximum (the derivative changes sign).

below P_c to be $P_{HD}/P_c = \frac{\sqrt{3}}{2}\Omega - \frac{1}{2}$ (dashed line). They are also shown on a plot of the output power in the inset of Fig. 4. There, $dP_{out}/d\omega_d$ is normalized to its maximum and plotted as a function of the drive frequency and power. The maximum output power (below P_c) is shown as a white line defined by $P_{max}/P_c = \frac{9}{8\sqrt{3}}\Omega$ and coincides with the change of sign of $dP_{out}/d\omega_d$. Note that these measurements do not probe the hysteresis since the fre-

quency is swept only in the forward direction. To verify the hysteretic behavior of the phenomenon, we used triangular power sweeps for several frequencies. We were able to probe the power and frequency dependence of both bifurcation points. The resulting data is shown as stars on Fig. 4. The deviation from predictions is most likely due to the proximity of the lower bifurcation current amplitude to I_0, situation not well addressed by the Duffing model. Note that the upper and lower bifurcation current in this RF experiment correspond to the switching and retrapping current, respectively, in DC Josephson IV measurement.

We now discuss how, from the measured value P_c of the critical power, we can infer I_0. In contrast to a DC experiment, where one can characterize the biasing circuit with great precision, an absolute calibration of the environmental impedance $Z(\omega)$ at RF frequencies is arduous. From the values of C_{in}, Z_0, L and Q obtained from the low power (linear) measurements, as well as the relations $V_{d\ crit} = \frac{V_C}{Z_0 C_{in}\omega_0}$ and $V_c = \frac{8}{3^{3/4}}(\frac{L+L_J}{L_J Q})^{3/2}\varphi_0\omega_0$, we extract $I_0 = \varphi_0/L_J$ from the measured value of $P_c = V_{d\ crit}^2/2R_L$. In table 1 we show that I_0 obtained in this way is consistent with the normal resistance test of junctions fabricated in the same batch. We can thus verify that the Duffing model hypothesis $I_c/I_0 = \frac{4}{\sqrt[4]{3}}\sqrt{\frac{L+L_J}{L_J}\frac{1}{Q}} \ll 1$ for the RF critical current amplitude I_c is well satisfied [11].

Other experiments on an AC biased Josephson junction have been realized [5, 12, 13, 14], albeit with a lower degree of control over the electrodynamic environment. Nonlinear effects involving superconducting weak links in resonators have been reported [15, 16, 17]. Moreover, the Duffing oscillator physics has been shown to appear in several other systems including nanomechanical resonators [18] and relativistic electrons [19]. However, our realization offers an unprecedented opportunity to study dynamical driven systems in the regime where quantum fluctuations are dominant [9], [20]. This regime is yet unexplored experimentally.

The excellent overall agreement between experimental results and theoretical predictions allows us to eliminate non-linear dissipative effects as the cause for the bifurcation. For instance, if the dissipation in the resonator would increase with power the resonance would become broader, its maximum would decrease and the resonance curves will eventually cross each other, an effect never observed in our experiment.

The main application we envisage in the short term for this phenomenon is parametric amplification at microwave frequency which would reach the quantum limit at the practical level, not simply at the proof-of-principle level. It could also used as a superconducting quantum bit readout [21]. Because the cavity frequency is mainly determined by geometry, we can stage in the frequency domain several cavities and multiplex the measurement or readout of a collection of entities.

In conclusion, we have observed the dynamical bifurcation of a superconducting microwave cavity incorporating a non-linear element in the form a Josephson tunnel junction. This bifurcation is analogous to the optical bistability observed with atoms in a Fabry-Perot in QED experiments. Our system is therefore at the crossroads between the physics of dynamical systems and quantum optics. Our level of control on the various parameters of this bistable phenomenon opens the door to amplification at the quantum limit, squeezing and other analog quantum information processing functions in the strong and ultra-strong coupling regimes.

* Present address: Département de Physique, Université de Sherbrooke, Canada
† Present address: Department of Physics, University of California, Berkeley, CA, USA
‡ Present address: Department of Physics, ETH Zurich, Switzerland
[1] A. D. Clerk PRL, S. M. Girvin and A. D. Stone, Phys. Rev. B **67**, 165324 (2003); U. Gavish, B. Yurke and Y. Imry, Phys. Rev. Lett. **93**, 250601 (2004).
[2] P. K. Day *et. al.*, Nature **425**, 817 (2003) and references therein.
[3] M. H. Devoret and R. J. Schoelkopf, Nature, **406**, 1039 (2000)
[4] C. M. Caves, Phys. Rev. D **26**, 1817 (1982)
[5] B. Yurke *et. al.*, Phys. Rev. A **39**, 2519 (1989).
[6] A. Wallraff *et. al.*, Nature **431**, 162, (2004).
[7] G. Rempe *et. al.*, Phys. Rev. Lett. **67**, 1727 (1991).
[8] L. Frunzio *et. al.*, IEEE Trans. Appl. Supercon. **15**, 860 (2005)
[9] M. A. Armen and H. Mabuchi, Phys. Rev. A **73**, 063801 (2006)
[10] I. Siddiqi *et. al.*, Phys. Rev. Lett., **94**, 027005 (2005).
[11] V.E. Manucharyan, *et. al.*, cond-mat 0612576
[12] I. Siddiqi *et. al.*, Phys. Rev. Lett. **93**, 207002 (2004).
[13] A. Lupascu *et. al.*, Phys. Rev. Lett. **96**, 127003 (2006).
[14] Janice C. Lee *et. al.*, IEEE. Trans. Appl. Supercon. **15**, 841 (2005).
[15] C.C. Chin *et. al.*, Phys. Rev. B **45**, 4788 (1992).
[16] B. Abdo *et. al.*, Phys. Rev. B **73**, 134513 (2006).
[17] E. A. Tholen *et. al.*, cond-mat 0702280
[18] J.S. Aldridge and A.N. Cleland, Phys. Rev. Lett. **94**, 156403 (2005); Stav Zaitsev *et. al.*, cond-mat/0503130.
[19] C.H. Tseng *et. al.*, Phys. Rev. A **59**, 2094 (1999).
[20] M.I. Dykman and V.N. Smelyanskii, Zh. Eksp. Teor. Fiz. **94**, 61 (1988).
[21] I. Siddiqi *et. al.*, Phys. Rev. B **73**, 054510 (2006).